DRFC-SCP-STGI EUR-CEA-FC-1253

IDENTIFICATION OF KRYPTON Kr XVIII TO Kr XXIX SPECTRA EXCITED IN TFR TOKAMAK PLASMAS

J.F. Wyart and TFR Group

February 1985

Submitted for publication in Physica Scripta.

IDENTIFICATION OF KRYPTON Kr XVIII TO Kr XXIX SPECTRA EXCITED IN TFR TOKAMAK PLASMAS

J.F. Wyart

Laboratoire Aimé Cotton, Bât. 505, CNRS II
Campus Universitaire, F-91405 Orsay-Cedex (France)

TFR Group
Association EURATOM-CEA sur la Fusion Contrôlée, B.P. n°6
F-92260 Fontenay-aux-Roses (France)

ABSTRACT

The emission spectrum of krypton (injected into TFR tokamak plasmas) has been recorded photographically in the 15-300 Å spectral range by means of a 2m grazing incidence spectrograph. Preliminary identification work, based on isoelectronic regularities from known spectra of other ions and ionization equilibrium calculations, has allowed 48 lines (belonging to the O I, F I, Na I, Mg I, Al I, Ar I and K I sequences) to be identified.

P.A.C.S. n° : 32.20

1. INTRODUCTION

Spectroscopic data on the spectra of multicharged ions for elements not of interest to astrophysics are very scarce and generally concern only a few simple isoelectronic sequences. However, rare gases are interesting elements for diagnostics purposes in tokamaks, since they do not pollute the vacuum vessel and are easily introduced into the plasma. We have therefore injected several rare gases into keV electron temperature TFR tokamak plasmas and, beside using routine spectroscopic diagnostics, have also photographically recorded their spectra in the far V.U.V. and soft x-ray spectral range down to ∿ 10 Å.

We report here the first results on line identification of highly ionized krypton ions. The spectrum of Kr is not completely unknown ; indeed, Hinnov [1] has identified in the PLT tokamak three resonance lines of sodium-like Kr XXVI and magnesium-like Kr XXV. Moreover, two spectroscopic studies at relatively low spectral resolution have been recently performed on lines from multicharged krypton ions produced either by electron beam bombardment of Kr gas [2] or in a theta-pinch plasma [3].

2. EXPERIMENTAL CONDITIONS

The experiments described here were performed on ohmically heated TFR tokamak plasmas. The plasma parameters, during the quasi-stationary current plateau phase, were the following : plasma current I_p = 180 kA, toroidal magnetic field B_T = 4.0 T, working gas H_2, graphite limiter radius a = 19.5 cm, central electron density $n_e(o) = 5 \times 10^{13}$ cm^{-3} and central electron temperature $T_e(o) = (1.4 \pm 0.15)$ keV. The impurity evolution, with both spatial and temporal resolution, was obtained above 100 Å using a V.U.V. duochromator equipped with a rotating mirror [4]. In addition, photographic spectra in the 10-300 Å spectral range were recorded by using a 2 m, grazing (1.5°) incidence spectrograph [5,6]. Two exposures were made : the first one, using a 600 groove /mm Jobin-Yvon holographic grating, covered the spectral region below 320 Å ; the second one, using a 2400 groove/mm, gold coated, 1° blazed Bausch and Lomb grating, covered the 10–100 Å spectral range. In both cases the line of sight of the spectrograph passed through the plasma center, and the number of discharges recorded on each plate was ∿ 100 (for each discharge a fast shutter limited the exposure time to the krypton puff duration). Wavelengths of intrinsic impurity lines (C,N,O,Cr,Fe, and Ni) were used as internal standards in order to derive the krypton line wavelengths by polynomial fitting (note also that comparison with plates obtained without krypton injection allows the krypton lines to be more easily picked-up). Above 100 Å the estimated accuracy was between 0.015 Å and 0.03 Å, depending on the intensity and profile of the considered line ; below 100 Å the uncertainty was estimated to be 0.015 Å.

Krypton was puffed into the plasma 60 ms after breakdown of the working gas (resulting in a increase of both the electron density and temperature), and was switched off after 300 ms. The V.U.V. duochromator was used to monitor resonance lines of peripheral low ionization potential ion (Kr VII, Zn-like sequence, $4s^2\ ^1S_o - 4s4p\ ^1P_1$, 585.4 Å, and Kr VIII, Cu-like sequence, $4s\ ^2S_{1/2} - 4p\ ^2P_{1/2,\ 3/2}$, 695.9 Å and 651.6 Å), and quasi-central medium ionization potential ions (Kr XXV, Mg-like sequence, ionization potential χ_i = 1150 eV, $3s^2\ ^1S_o - 3s\,3p\ ^1P_1$, 158.2 Å, and Kr XXVI, Na-like sequence, χ_i = 1205 eV, $3s\ ^2S_{1/2} - 3p\ ^2P_{1/2,\ 3/2}$, 220 Å and 179 Å), already identified by Hinnov [1] .

Figure 1 shows the temporal evolution of the plasma current I_p, the central electron temperature $T_e(0)$ (obtained from the second harmonic of the electron cyclotron emission), the central electron density $n_e(o)$ (derived from multichannel HCN laser interferometry after Abel inversion), and the radiance B_z of the Kr XXV 179 Å line. The duration of the krypton puff is shown by the two vertical dashed lines.

Figure 2 a and b show, at 200 ms, the radial profiles of T_e (from Thomson scattering), n_e, and the Kr^{24+} and Kr^{25+} ion densities ; the latter, normalized to their peak values, are deduced from emissivities (i.e. Abel inverted radiances) E_z of the Kr XXV 158.2 Å and Kr XXVI 179 Å lines. During the quasi-stationary current plateau phase the radial profiles did not vary, only the absolute values of the emissivities increasing due to both the electron density increase and the incoming krypton flux.

The peak emissivity of the Kr XXVI 179 Å line reached (4-6) x 10^{14} photons cm^{-3} s^{-1} at the end of the puffing. Using the interpolated values of Weiss [7] for the oscillator strength and the $\bar{g}$-approximation for the excitation rate coefficient, this leads to a central Kr^{25+} ion density of (3-5) x 10^9 cm^{-3}, from which a total central krypton density of (1-2) x 10^{10} cm^{-3} can be inferred.

Figure 2c shows a plot of the calculated fractional abundances $f_z (= n_z / \Sigma n_z)$ for the central krypton ions ; these calculations assume ionization-recombination equilibrium and use an up-to-date atomic data package, including auto-ionization when important [8,9] . A comparison between experimental ion density profiles and calculated fractional abundances shows that the krypton ions are somewhat more central than predicted by the ionization equilibrium model. This is not surprising, since it is well known that the inward impurity diffusion must also be considered, resulting in a decrease of the average charge state by approximately 0.5-1 [10] . In any case, this type of calculations indicates that the highest charge state existing with non-negligible abundance in the plasmas considered here is Kr^{28+}. Any identification of spectral lines emitted by ions with higher charge, based only on atomic structure calculations or empirical isoelectronic regularities, must therefore be dismissed. As an example, a line at 72.675 Å which could have been identified as the transition $2s^2\ ^1S_0 - 2s\ 2p\ ^1P_1$ of Kr XXXIII predicted at 72.65 Å certainly belongs to a lower ionization stage.

A portion of an experimental spectrum between 132 and 160 Å is shown in figure 3, where some of the most intense lines (of both krypton and intrinsic impurities, i.e ; C,O,Cr,Fe, and Ni) are explicitly identified.

3 . INTERPRETATION OF THE SPECTRA

Line identification after wavelength determination by polynomial fitting, has been performed using one (or several) of the following methods :

i) - comparison of measured wavelengths with semi-empirical predictions by Edlen in the sequences of O I, F I [11], and Na I [12] .

ii) empirical interpolations or extrapolations of wavenumbers (expressed as an adjustable polynomial in Z_c^n, Z_c being the net charge of the core) along isoelectronic sequences previously investigated.

iii) parametric studies of electronic configurations by the Slater-Condon method (the electrostatic and spin-orbit parameters being scaled Hartree-Fock radial integrals) ; systematic trends of the scaling factors, determined for each parameter for the well known first members of the isoelectronic sequence under study, are then extrapolated to krypton.

The 48 lines classified so far are listed in table I, together with intensity estimates from a densitometer tracing of the plates. In the last columns of table I are given successively the spectrum, the combining levels, along with numerical values or references for earlier predictions or observations. The energy levels derived from the classified lines are reported in table II.

In the following, we shall comment on some of the identifications, by order of increasing ionization state.

3.1. Kr XVIII

The isoelectronic sequence of K I consists of one-electron configurations $3p^6$ nl which overlap and mix with core-exited configurations such as $3p^5$ $3d^2$ and $3p^5$3d4s. As shown by Ramonas and Ryabtsev [13], $3p^5 3d^2$ is the lowest odd configuration for elements with Z $\geqslant$ 28. The strongest $3p^6$3d - $3p^5 3d^2$ transitions have been traced up to Ge XIV [14] .

For $Z > 32$, these have not been identified in the large $3p^6 3d^N - 3p^5\ 3d^{N+1}$ transition arrays which overlap each other for different values of N. By combining methods ii) and iii) outlined above, the transition array $3p^6\ 3d - 3p^5\ 3d^2$ can be predicted. It involves a few very strong lines which have been identified and many weak lines merging in the bulk of all 3p - 3d transitions. In all known potassium-like ion spectra, the ratio of the measured splitting of the ground term 3d ^2D to the ab-initio value derived from Hartree-Fock integrals displays a smooth evolution as a function of Z and the derived estimate for Kr XVIII (15710 ± 60 cm^{-1}) lies in the middle of the wavenumber differences for three couples of lines arising from $3p^5 (^2P)\ 3d^2(^3F)\ ^2D_{3/2,5/2}$ and $3p^5(^2P)\ 3d^2(^3P)\ ^2P_{3/2}$

It is expected that the $3p^6\ 3d - 3p^6\ 4f$ transition involves the strongest lines of the one-electron system. The two lines identified on the basis of interpolation between elements with $Z \leqslant 33$ and $Z = 42$ (Mo XXVI [15]) display a satisfactory intensity ratio, but lead to an inverted 4f ^2F doublet (fine structure - 900 cm^{-1}). Due to the fact that $3p^6$ 4f may be surrounded and pertrubed by core-excited levels and due to the absence of alternative lines, this inversion does not rule out the present identification.

3.2. Kr XIX

The highest level of the first excited configuration of multi-charged argon-like ions, $3p^5 3d$, allows a very strong line $3p^6\ ^1S_0 - 3p^5\ 3d\ ^1P_1$ (which had been traced up to Ge XV [14]) to be identified. Indeed, the extrapolated wavenumber for Kr XIX fits an intense line observed at 96.263 Å. The energy interval $^1P_1 - ^3D_1$ in $3p^5 3d$ was estimated by means of method (iii). As the recorded spectrum is very dense near 120 Å, the identification of the transition $3p^6\ ^1S_0 - 3p^5 3d\ ^3D_1$ reported on table I may be considered as tentative. In this spectral region some of the lines probably belong to the $3p^{N+1} - 3p^N 3d$ (N=1-4) transition arrays of Kr XX-XXIII, needing further identification work.

3.3. Kr XXIV

Three lines in the Al I isoelectronic sequence have been previously traced up to As XXI or Se XXII [14]. Krypton lines of medium or strong intensity are found at the extrapolated wavelengths. By combination with two other lines at 130.714 Å and at 134.100 Å they lead to a ground - term interval of 97420 cm^{-1} for Kr XXIV $3s^2 3p\ ^2P_{3/2,1/2}$, which is very close to the recently predicted values of 97196 cm^{-1} [16] and 97320 cm^{-1} [17].

3.4. Kr XXV

The resonance line $3s^2\ ^1S_0 - 3s3p\ ^1P_1$ of the magnesium-like ion is the strongest krypton line present on our spectra ; the other strong transitions, observed by Reader in the sequence Sr XXVII-Rh XXXIV [18], namely $3s3p\ ^3P_2 - 3s3d\ ^3D_3$ and $3s3p\ ^1P_1 - 3s3d\ ^1D_2$, are well excited also in the tokamak plasmas. The intercombination line $3s^2\ ^1S_0 - 3s3p\ ^3P_1$ which has been observed in the PLT tokamak for seven elements between scandium and molybdenum, is now measured in Kr XXV at 242.550 ± 0.030 Å, i.e. close to the predicted interpolated value of 242.4 Å [19]. The intensity of the lines mentioned above allowed us to search for the weaker transitions predicted by Cheng and Johnson [20]. However, due to a lack of available data in the spectra of neighbouring elements, some of the identifications still need to be confirmed by isoelectronic regularities.

3.5. Kr XXVI

The isoelectronic sequence of sodium-like ions has been extensively studied both experimentally and theoretically [12,21]. Empirical extrapolations for n=4 to n=5 transitions and interpolations for n=3 to n=4 transitions (Mo XXXII being known [15]), lead to wavelengths which are within the experimental uncertainty of our measurements. The Edlén predictions for n=3 to n=3 transitions [12] are also confirmed.

3.6. Kr XXVIII and Kr XXIX

By means of a smooth fitting of the discrepancies between experimental and ab-initio relativistic energy levels, Edlén [11] recently predicted the levels of $2s^m\ 2p^n$ configurations for multicharged ions, including krypton, in the isoelectronic sequences of Li I, Be I, B I, N I, O I and F I. Some lines reported in Table I support these predictions.

The couple of lines $2s^2 2p^5\ ^2P_{1/2,3/2} - 2s2p^6\ ^2S_{1/2}$ observed at 52.584 and 68.734 Å lead to a ground state interval of 446800 ± 500 cm^{-1} for the fluorine-like krypton and imply existence of a magnetic dipole transition at 223.81 ± 0.25 Å, which agrees with four different predictions [11] and all in the range 224.00 ± 0,05 Å. The closest line which we can attribute to krypton is at 223.682 Å, but it is difficult to conclude at this early stage that it is the M1 transition. Finally, three lines of oxygen-like krypton display much weaker intensity than Kr XXVIII lines, in agreement with the ionization equilibrium calculation.

4. CONCLUSION

A preliminary analysis of the krypton spectrum excited in the plasma of the TFR tokamak has allowed a substantial extension of line identifications in Kr XXV and Kr XXVI, as well as identifications in Kr XVIII, Kr XIX, Kr XXIV, Kr XXVIII, and Kr XXIX. The availability of routine spectroscopic diagnostics of the plasmas considered here, together with the use of a numerical ionization equilibrium code, has permitted to confirm the existence of these ionization stages, at the same time showing that higher ionization degrees cannot be present with sufficient densities to be observed. Identification of many weak lines will require isoelectronic comparisons with the spectra of near-by elements and extended theoretical studies of the level structure for these ions.

Acknowledgement

The authors wish to thank Dr. J.L. Schwob for his help in the operation of the spectrograph.

REFERENCES

[1] HINNOV E., Phys. Rev. A 14, 1533 (1976)

[2] BLEACH R.D., J. Opt. Soc. Am. 70, 801 (1980) ; see also BLEACH R.D., NAGEL D.J., DUKART R., and DIETRICH D., Proceed. 7th Int. Conf. on Vacuum Ultraviolet Radiation Physics, Jerusalem, Israël (1983)

[3] JONES D.A., and KALLNE E., J. Quant. Spectrosc. Radiat. Transfer 30, 317 (1983)

[4] BRETON C., DE MICHELIS, C., FINKENTHAL M, and MATTIOLI M., J. Phys. E : Sci. Instrum. 12, 894 (1979)

[5] BRETON C., DE MICHELIS C., FINKENTHAL M. and MATTIOLI M., J. Opt. Soc. Am. 69, 1652 (1979)

[6] TFR GROUP, DOYLE J.G., SCHWOB J.L., J. Phys. B : At. Mol. Phys. 15, 813 (1982)

[7] WEISS A.W., J. Quant. Spectrosc. Radiat. Transfer 18, 481 (1977)

[8] BRETON C., COMPANT LA FONTAINE A, DE MICHELIS C., HECQ W., LASALLE J. LECOUSTEY P., MATTIOLI M., MAZZITELLI G., PLATZ P. and RAMETTE J; J. Phys. B : At. Mol. Phys. 16, 2627 (1983).

[9] BRETON C., DE MICHELIS C, HECQ W., MATTIOLI M., RAMETTE J. and SAOUTIC B. Plasma Phys. Control. Fusion (1985, in press)

[10] TFR GROUP, Nucl. Fusion 23, 539 (1983)

[11] B. EDLEN, Physica Scripta 28, 5 (1983)

[12] B. EDLEN, Physica Scripta 17, 565 (1978)

[13] RAMONAS A.A. and RYABTSEV A.N., Opt. Spectrosc. 48, 348 (1980)

[14] FAWCETT B.C., and HAYES R.W., J. Opt. Soc. Am. 65, 623 (1975)

[15] SCHWOB J.L., KLAPISCH M., SCHWEITZER N., FINKENTHAL M., BRETON C., DE MICHELIS C. and MATTIOLI M., Phys. Lett. 62A, 85 (1977)

[16] CURTIS L.J. and RAMANUJAM P.S., Physica Scripta 27, 417 (1983)

[17] SUGAR J., and KAUFMAN V., J. Opt. Soc. Am. B1, 218 (1984)

[18] READER J., J. Opt. Soc. Am. 73, 796 (1983)

[19] FINKENTHAL M., HINNOV E., COHEN S., and SUCKEWER S., Phys. Lett. 91, 284 (1982)

[20] CHENG K.T. and JOHNSON W.R., Phys. Rev. A16, 263 (1977)

[21] KONONOV E. Ya, RYABTSEV A.N., and CHURILOV S.S., Physica Scripta 19, 328 (1979)

[22] SHORER ᵖ., LIN C.D., and JOHNSON W.R., Phys. Rev. A16, 1109 (1977)

FIGURE CAPTIONS

Fig. 1 Time evolutions of : a) plasma current I_p ; b) central electron density $n_e(o)$ (dashed line) and central electron temperature $T_e(o)$ (solid line, normalized to the value ∲ given by Thomson scattering at t = 200 ms) ; and c) Kr XXVI 179 Å line radiance B_z. The hatched interval between the vertical dashed lines show the krypton injection time.

Fig. 2 Radial profiles at t = 200 ms of : a) electron density $n_e(r)$ (solid line) and electron temperature $T_e(r)$ (dashed line) ; b) normalized Kr^{25+} and Kr^{24+} ion densities $n_z(r)$ deduced from the KrXXVI 179 Å and KrXXV 158.2 Å emissivities ; and c) fractional abundances of central krypton ions $f_z(r)$ at ionization equilibrium. The horizontal error bar on b) indicates the shot-to-shot variation of the positions of the maxima of the emissivities.

Fig. 3 Densitometer tracing of the TFR spectrum with krypton injection in the 132-160 Å spectral range (the line quoted (e) around 152 Å is probably a blending of Kr and intrinsic impurity lines).

TABLE I CLASSIFIED LINES OF Kr XVIII - Kr XXIX

Wavelength Å	Intensity	Spectrum	Classification	Previous observation	Previous prediction	Present empirical prediction
21.185	15	XXVI	$3s\ ^2S_{1/2} - 4p\ ^2P_{3/2}$	[2]		21.186
21.369	10	XXVI	$3s\ ^2S_{1/2} - 4p\ ^2P_{1/2}$	[2]		21.363
21.840	5 p	XXV	$3s^2\ ^1S_o - 3s\ 4p\ ^1P_1$		21.858 [22]	21.853
22.257	5	XXVI	$3p\ ^2P_{1/2} - 4d\ ^2D_{3/2}$	[2]		22.259
22.743	10	XXVI	$3p\ ^2P_{3/2} - 4d\ ^2D_{5/2}$	[2]		22.742
24.766	10 p	XXVI	$3p\ ^2P_{1/2} - 4s\ ^2S_{1/2}$	[2]		
25.416	30	XXVI	$3p\ ^2P_{3/2} - 4s\ ^2S_{1/2}$	[2]		
25.621	30	XXVI	$3d\ ^2D_{3/2} - 4f\ ^2F_{5/2}$	[2]		25.623
25.729	40	XXVI	$3d\ ^2D_{5/2} - 4f\ ^2F_{7/2}$	[2]		25.732
35.190	10	XVIII	$3p^6 3d\ ^2D_{3/2} - 3p^6 4f\ ^2F_{5/2}$			
35.397	20	XVIII	$3p^6 3d\ ^2D_{5/2} - 3p^6 4f\ ^2F_{7/2}$			
52.584	25	XXVIII	$2s^2\ 2p^5\ ^2P_{3/2} - 2s 2p^6\ ^2S_{1/2}$		52.589 [11]	
53.612	2	XXIX	$2s^2 2p^4\ ^3P_2 - 2s 2p^5\ ^3P_1$		53.631 [11]	
53.977	4 w	XXIX	$2s^2 2p^4\ ^1D_2 - 2s 2p^5\ ^1P_1$		53.975 [11]	
59.377	6	XXVI	$4f\ ^2F_{5/2} - 5g\ ^2G_{7/2}$			

58.459	8	XXVI	$4f\ ^2F_{7/2} - 5g\ ^2G_{9/2}$			
59.684	4	XXIX	$2s^22p^4\ ^3P_2 - 2s2p^5\ ^3P_2$		59.689 [11]	
68.734	10	XXVIII	$2s^22p^5\ ^2P_{1/2} - 2s2p^6\ ^2S_{1/2}$		68.728 [11]	
91.391	5	XVIII	$3p^63d\ ^2D_{3/2} - 3p^53d^2\ ^2P_{3/2}$			
92.005	3	XVIII	$3p^63d\ ^2D_{3/2} - 3p^53d^2\ ^2D_{5/2}$			
92.225	25	XVIII	$3p^63d\ ^2D_{3/2} - 3p^53d^2\ ^2D_{3/2}$			
92.728	25	XVIII	$3p^63d\ ^2D_{5/2} - 3p^53d^2\ ^2P_{3/2}$			
92.956	18	XVIII	$3p^63d\ ^2D_{3/2} - 3p^53d^2\ ^2P_{1/2}$			
93.353	30	XVIII	$3p^63d\ ^2D_{5/2} - 3p^53d^2\ ^2D_{5/2}$			
93.569	2	XVIII	$3p^63d\ ^2D_{5/2} - 3p^53d^2\ ^2D_{3/2}$			
96.263	45	XIX	$3p^6\ ^1S_0 - 3p^53d\ ^1P_1$			
110.242	10 p	XXV	$3s3d\ ^1D_2 - 3s3p\ ^3P_1$			
118.546	15	XIX	$3p^6\ ^1S_0 - 3p^53d\ ^3D_1$			
118.603	40	XXIV	$3s^23p\ ^2P_{1/2} - 3s^2\ 3d\ ^2D_{3/2}$			113.606
129.895	15 p	XXV	$3s3p\ ^3P_1 - 3s3d\ ^3D_2$			
130.714	30	XXIV	$3s^23p\ ^2P_{1/2} - 3s3p^2\ ^2P_{3/2}$			
131.808	45	XXIV	$3s^23p\ ^2P_{3/2} - 3s^23d\ ^2D_{5/2}$			131.421
134.100	20	XXIV	$3s^23p\ ^2P_{3/2} - 3s^23d\ ^2D_{3/2}$			
140.877	25	XXVI	$3p\ ^2P_{1/2} - 3d\ ^2D_{3/2}$		140.878 [12]	

141.643	23	XXV	$3s3p\ ^3P_2 - 3s3d\ ^3D_3$			141.645
144.665	16	XXV	$3s3p\ ^3P_2 - 3s3d\ ^3D_2$			
145.498	23	XXV	$3s3p\ ^1P_1 - 3s3d\ ^1D_2$			145.521
149.785	40 p	XXIV	$3s^23p\ ^2P_{3/2} - 3s3p^2\ ^2P_{3/2}$			149.284
158.214	75	XXV	$3s^2\ ^1S_o - 3s3p\ ^1P_1$	159.0 [1]	158.10 [18]	158.160
159.925	30	XXVI	$3p\ ^2P_{3/2} - 3d\ ^2D_{5/2}$		159.889 [12]	
166.078	12	XXV	$3s3p\ ^3P_2 - 3p^2\ ^3P_2$		164.6 [20]	
168.664	6	XXV	$3s3p\ ^3P_1 - 3p^2\ ^3P_1$		167.9 [20]	
179.085	70	XXVI	$3s\ ^2S_{1/2} - 3p\ ^2P_{3/2}$	179.6 [1]	178.965 [12]	
194.444	20	XXV	$3s3p\ ^3P_2 - 3p^2\ ^3P_1$		193.2 [20]	
197.620	5	XXV	$3s3p\ ^3P_2 - 3p^2\ ^1D_2$			
220.058	50	XXVI	$3s\ ^2S_{1/2} - 3p\ ^2P_{1/2}$	220.6 [1]	220.032 [12]	
242.550	15	XXV	$3s^2\ ^1S_o - 3s3p\ ^3P_1$		242.4 [19]	242.624
274.170	5	XXV	$3s3p\ ^1P_1 - 3s3d\ ^1D_2$			

Note : p , perturbed by close line ; w , wide line

TABLE II Energy levels of multicharged krypton ions

Configuration	Term	J	Energy (cm^{-1})
Kr XVIII			
$3p^6\ 3d$	^2D	3/2	0
	^2D	5/2	15700
$3p^5\ 3d^2$	$(^3P)\ ^2P$	1/2	1075 800
	$(^3F)\ ^2D$	3/2	1084 300
	$(^3F)\ ^2D$	5/2	1086 900
	$(^3P)\ ^2P$	3/2	1094 200
$3p^6\ 4f$	^2F	7/2	2 840 800
		5/2	2 841 700
Kr XIX			
$3p^6$	^1S	0	0
$3p^5\ 3d$	^3D	1	844 200
	^1P	1	1 038 800
Kr XXIV			
$3s^2\ 3p$	^2P	1/2	0
		3/2	97 420
$3s\ 3p^2$	^2P	3/2	765 040
$3s^2\ 3d$	^2D	3/2	843 140
		5/2	856 100
Kr XXV			
$3s^2$	^1S	0	0
$3s3p$	^3P	1	412 286
		2	490 900

	^1P	1	632 055
$3p^2$	^1D	2	996 850
	^3P	1	1 005 180
		2	1 093 030
3s3d	^3D	2	1 182 140
		3	1 196 900
	^1D	2	1 319 350
Kr XXVI			
3s	^2S	1/2	0
3p	^2P	1/2	454 430
		3/2	558 550
3d	^2D	3/2	1 164 270
		5/2	1 183 840
4s	^2S	1/2	4 493 000
4p	^2P	1/2	4 697 700
		3/2	4 720 300
4d	^2D	3/2	4 947 400
		5/2	4 955 500
4f	^2F	5/2	5 067 300
		7/2	5 070 500
5g	^2G	7/2	6 751 500
		9/2	6 752 300
Kr XXVIII			
$2s^2\ 2p^5$	^2P	3/2	0
		1/2	446 800
$2s\ 2p^6$	^2S	1/2	1 901 700

Kr XXIX (a)			
$2s^2\ 2p^4$	^3P	2	0
	^1D	2	525 066 + x
$2s\ 2p^5$	^3P	2	1 675 500
		1	1 865 300
	^1P	1	2 377 700 + x

Note : a) the singlet system being not connected to the ground level, the $^1D_2$ level was taken from [11] .

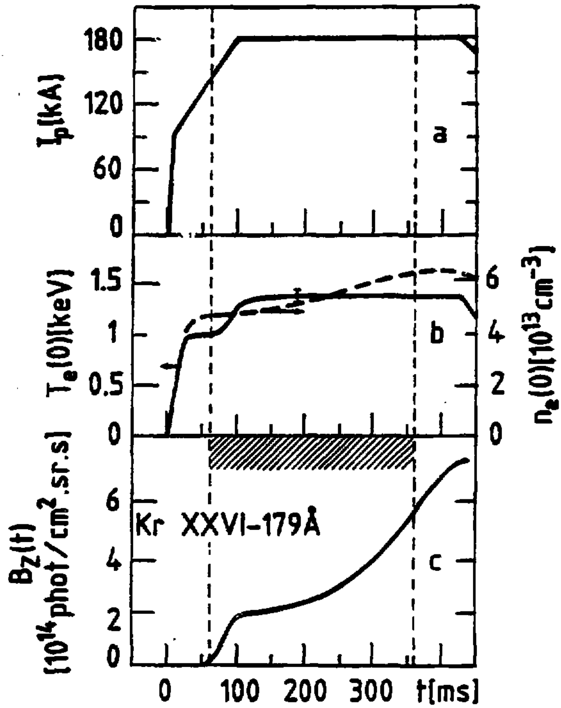

180
120
60
0
I_p(kA)
a
1.5
1
0.5
0
$T_e(0)$(keV)
6
4
2
0
$n_e(0)(10^{13}cm^{-3})$
b
6
4
2
0
$B_Z(t)$
$(10^{14}$phot/cm^2.sr.s)
Kr XXVI-179Å
c
0
100
200
300
t(ms)

Fig. 1

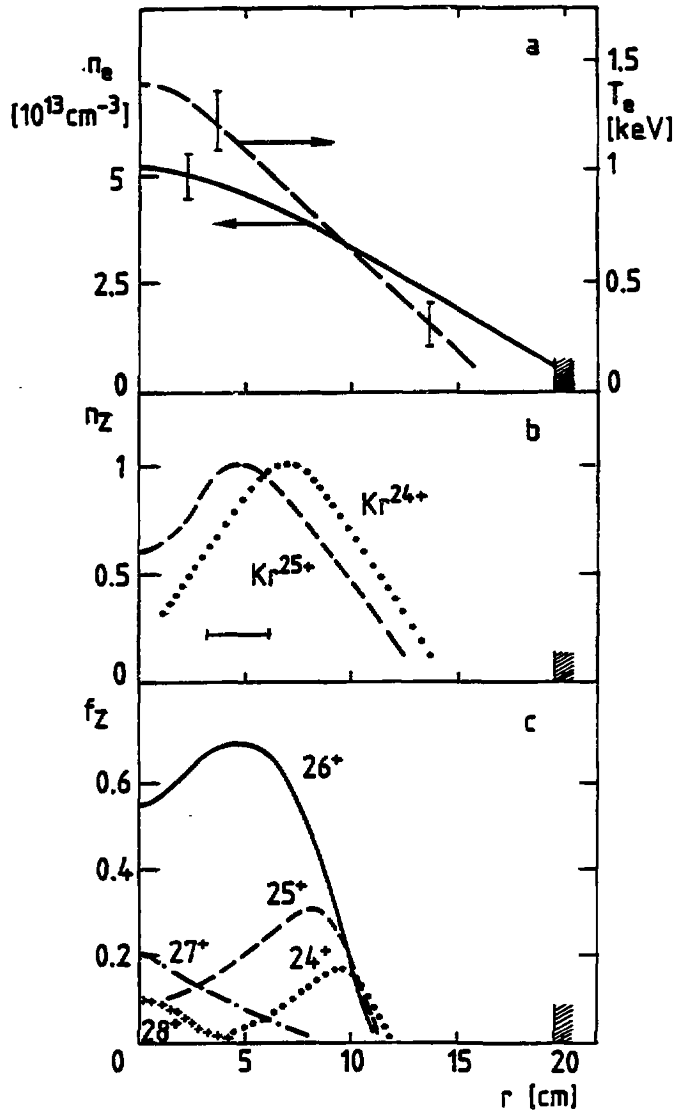

a
n_e
$[10^{13} cm^{-3}]$
5
2.5
0
1.5
T_e
[keV]
1
0.5
0
b
n_Z
1
0.5
0
Kr^{24+}
Kr^{25+}
c
f_Z
0.6
0.4
0.2
0
26^+
25^+
27^+
24^+
28^+
5
10
15
20
r [cm]

Fig. 2

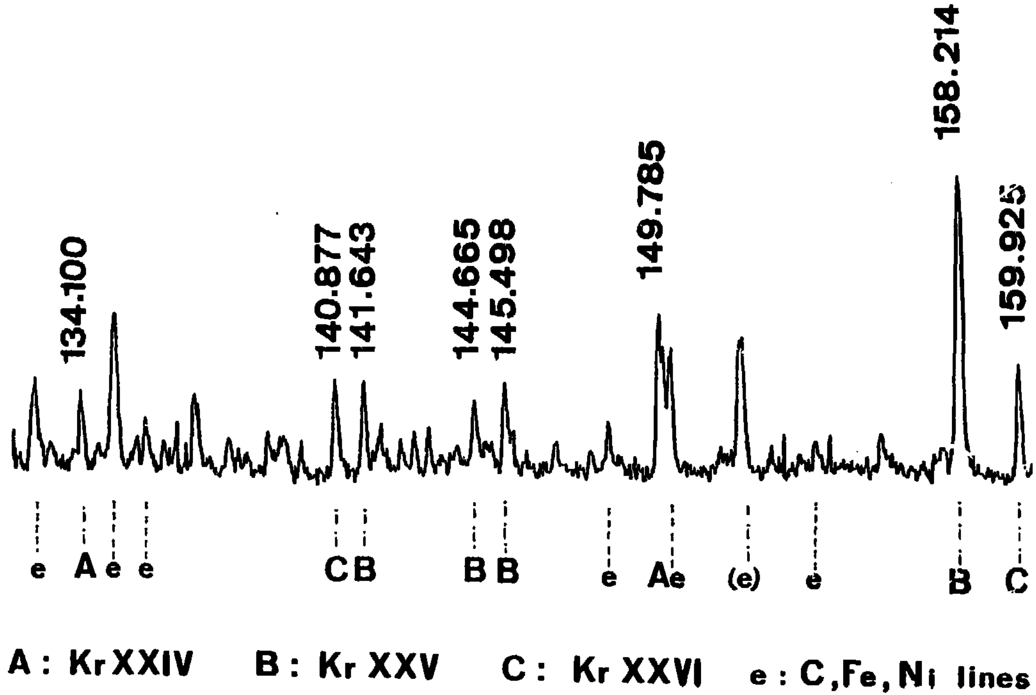

134.100
140.877
141.643
144.665
145.498
149.785
158.214
159.925
e A e e
C B
B B
e Ae (e) e
B C
A : Kr XXIV B : Kr XXV C : Kr XXVI e : C, Fe, Ni lines

FIG. 3

S C P

ÉQUIPE T.F.R.

LISTE N° 11 - MISE À JOUR DU 1ER. OCTOBRE 1984

EXPLOITATION PHYSIQUE DE L'EXPÉRIENCE

- COORDINATION.. M. CHATELIER
  J. TACHON
- SECRÉTARIAT SCIENTIFIQUE.............................. P. LECOUSTEY
- CONDUITE DE LA MACHINE................................ P. BANNELIER
  M. CHATELIER
  M. DUBOIS
  P. GIOVANNONI
  L. LAURENT
  J. TACHON
- MESURES MAGNÉTIQUES................................... J.L. DURANCEAU
  P. LECOUSTEY
- INTERFÉROMÉTRIE HCN................................... J.L. BRUNEAU
  D. VÉRON
- RÉFLECTOMÉTRIE.. M. CALDERON
  R. CANO
  F. SIMONET
- DIFFUSION THOMSON..................................... J. LASALLE
  P. PLATZ
- SPECTRES DE NEUTRES................................... T. HUTTER
  C. REVERDIN
- MESURES NUCLÉAIRES, X-DURS............................ A. GÉRAUD
  G. MARTIN
- RAYONS X-MOUS... L. JACQUET
  A.L. PECQUET
- SPECTROMÉTRIE (VISIBLE, UV, X-MOUS)................... C. BRETON
  C. DE MICHELIS
  W. HECQ
  M. MATTIOLI
  P. PLATZ
  J. RAMETTE
  B. SAOUTIC
- BOLOMÉTRIE.. M.H. ACHARD
- SPECTROMÉTRIE DE MASSE, CONDITIONNEMENT DES PAROIS, PLASMA PÉRIPHÉRIQUE................................... M.H. ACHARD
  A. GROSMAN
  F. LINET
- RAYONNEMENT CYCLOTRONIQUE ÉLECTRONIQUE
  - A) SPECTROMÉTRIE INFRAROUGE.......................... L. LAURENT
    R. SOUBARAS
  - B) ÉTUDES MICROONDES................................. R. CANO
    M. CALDERON
    B. ZANFAGNA

./...

- MESURE DE LA TURBULENCE PAR DIFFUSION THOMSON.......	H. BARKLEY B. DE GENTILE F. GERVAIS J. OLIVAIN A. QUEMENEUR L. PIGNOL
- SOURCE MODULÉE......................................	J. DRUAUX M. FOIS P. GIOVANNONI T. HUTTER
- INJECTION DE GLACONS................................	H. DRAWIN O. LAZARE

CHAUFFAGES ADDITIONNELS

- INJECTION DE NEUTRES................................	J.F. BONNAL J. DRUAUX M. FOIS P. GIOVANNONI R. OBERSON J.P. ROUBIN
- CHAUFFAGE CYCLOTRONIQUE IONIQUE.....................	J. ADAM P. BANNELIER R. BRUGNETTI A. FISSOLO D. GAMBIER H. KUUS
- CHAUFFAGE CYCLOTRONIQUE ÉLECTRONIQUE................	R. CANO J.P. CRENN M. DUBOIS L. REBUFFI B. TOURNESAC B. ZANFAGNA

INFORMATIQUE

- MATÉRIEL..	M. CHARET
- LOGICIEL..	J. BRETON A. COHEN C. REVERDIN J. TOUCHE
- THÉORIE...	J. ANDRÉOLETTI H. CAPES M. COTSAFTIS M. DUBOIS J. JOHNER E. MASCHKE M. PAIN A. SAMAIN